COBEM 2021 26th International Congress of Mechanical Engineering
ABCM Associação Brasileira de Engenharia e Ciências Mecânicas
November 22-26, 2021, Virtual Congress, Brazil

COB-2021-0770
FOAM GENERATION DURING GAS INVASION OF A POROUS MEDIUM SATURATED WITH SURFACTANT SOLUTION

Nicolle Lima
Sidnei Paciornik
Marcio Carvalho
Pontifical Catholic University of Rio de Janeiro (PUC-Rio)
nicolle@lmmp.mec.puc-rio.br
sidnei@puc-rio.br
msc@puc-rio.br

Abstract. *Foam has great potential to be used in oil recovery operations to improve sweep efficiency, in gas storage and acidization operations, and to solve problems caused by either a thief zone or gravity override. It can also be used in the remediation of contaminated sites. Foam, when produced in situ, fills the high permeability areas and diverts the displacing fluid into the direction of trapped oil, reducing the relative permeability of gas and leading to a more stable displacement front. The efficiency of these processes largely depends on the generation and stability of the foam films (lamellae) residing in the pores. The mobility of the injected gas is reduced when it's foamed; this reduction is attributed to the increase in the gas effective viscosity and the reduction in gas relative permeability. The liquid films formed create resistance against the gas flow, impeding its free motion inside the porous media. The lamellae population that composes the foam is directly related to surfactant concentration, and their flow and mobility are functions of the pore geometry and foam properties. However, the dynamics of foam formation in porous media and the relationship between the generation rate and pressure gradient as a function of surfactant concentration are not fully understood. The goal of this research is to understand the dynamic process of gas invading a two-dimensional porous media glass model occupied by a surfactant solution. A microfluidic setup composed of a glass micromodel that represents the porous medium, a syringe pump, a pressure transducer, and a microscope, was used to visualize the pore-scale displacement and correlate the evolution of lamellae formation during the injection process with pressure difference for different flow conditions through image processing. The dynamics of lamellae formation are reported and related to macroscopic flow behavior.*

Keywords: *porous media, microfluidics, EOR, foam*

1. INTRODUCTION

Gas commonly is injected in the reservoir to maintain the pressure and displace the oil towards production wells, but during gas injection, gas flows through the upper part of the reservoir by-passing large quantities of oil, and gas breakthrough from injection well to producing well occurs at a relatively high oil saturation. The poor sweep efficiency and displacement instabilities, known as viscous fingers, can be overcome with foam injection.

Foam can be injected into the subsurface or formed in situ during surfactant-alternating-gas injection to reduce the mobility of gas phase by increasing its effective viscosity and to divert the gas flow to low permeability regions (Boud and Holbrook (1958); Conn *et al.* (2014)). It is a technique that has been successfully used as an Enhanced Oil Recovery (EOR) method and in the remediation of contaminated sites (Hirasaki *et al.* (2000); Blaker *et al.* (2002); Portois *et al.* (2018)). And its success highly depends on generation and stability of liquid films residing in the pores.

Foam is a two-phase system in which gas is enclosed by surfactant-containing liquid films, called lamellae. It may contain more ou less liquid, a dry foam that has little liquid, consists basically of thin films. And as the fraction of liquid increases, foam reaches the other limit, in which it's called wet foam as can be seen in the Figure 1. The quantity of liquid films gives to the foam its texture and rheological properties.

Gas can present itself in different ways in a porous medium, trapped or flowing in a continuous or discontinuous phase (Kovscek and Radke (1993)). Trapped gas and gas bubbles resistance to flow provides a lower mobility comparing with flow of gas and liquid phases alone.

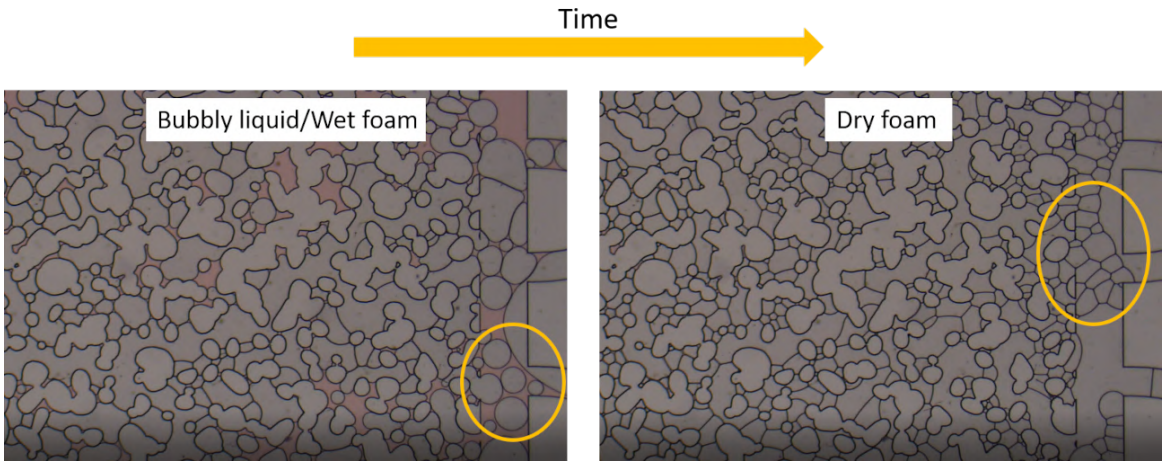

Figure 1. Liquid fraction in the beginning of the experiment and in the end

The most significant breakthrough in foam knowledge that has enabled foam mobility control to become a reality is a better understanding of the conditions required to generate strong foam. During surfactant solution and gas flow across homogeneous porous medium, a critical pressure gradient must be exceeded to form strong foam. (Rossen (1996); Tanzil *et al.* (2002); Gauglitz *et al.* (2002)). Gas may flow as a continuous phase below this pressure gradient. And above this pressure stationary bubbles are mobilized and flow in bubble trains. A bubble that is flowing can divide into two bubbles. If the critical pressure gradient required for strong foam is established, experiments can be carried out at a high enough flow rate or pressure drop to exceed the critical pressure gradient.

Other important advance is understanding that once the minimum pressure is achieved, the rate of foam generation in porous media is highly influenced by the surfactant concentration. This is most likely related to the rate at which lamellae are created and destroyed. As the surfactant concentration rises, the rate of foam generation rises as well (Kahrobaei and Farajzadeh (2019)).

In this publication, a study of foam generation through a porous medium using a microfluidic system is reported. Previous works studied surfactant concentration impact on foam behavior using core-flooding experiments (Kahrobaei and Farajzadeh (2019)) but not fully visualizing the dynamics. And the observation of foam evolution was carried out in another work but not evaluating the surfactant concentration impact (Li and Prigiobbe (2020)). To the best of authors' knowledge, this is the first study conducted to observe the effect of surfactant concentration on the foam generation and evolution counting the lamellae density during gas injection in a device completely saturated with surfactant solution.

2. MATERIALS AND METHODS

2.0.1 Surfactant

Surfactants, also known as surface active agents, are amphiphilic molecules consisting of a hydrophilic part, referred to as the head, and a hydrophobic part, referred as the tail. The surfactant head can be anionic, cationic, nonionic or zwitterionic. And the tail consists of linear or branched hydrocarbons chain. Aromatic groups and haloalkanes also may be present in the surfactant tails (Lin (2008)).

When dissolved in water, the amphiphilic feature of surfactants leads to the segregation of the hydrophobic tails from water and to the exposure of the hydrophilic heads, which results in the formation of aggregates above a threshold concentration, known as critical micelle concentration (CMC). Above the CMC the micelles coexist with single dispersed surfactant molecules, the monomers. And additional surfactants added to the system go to micelles (Lin (2008)).

In the experiments reported in this paper, we used sodium dodecyl sulfate (SDS), also known as sodium lauryl sulfate (SLS). It is an anionic surfactant (Vetec Quimica Fina) with formula $C_{12}H_{25}NaSO_4$, molecular weight of 288.38 g/mol and purity 90% in deionized water (18.2 MΩ cm). The solution was prepared by dissolving the powder surfactant in deionized water, filtrated through a 0.45μm filter. Aqueous dye was added to the surfactant solution to better distinguish liquid from other fluids and glass matrix in the visualization experiments.

Surface tension measurements were carried out in aqueous solutions of SDS in order to determine the CMC of the system. All measurements were done on a DCAT25 tensiometer by DataPhysics Instruments using a Wilhelmy plate. The reported values of the surface tension were obtained at constant temperature of 23^{o}C. The equilibrium surface tension of the pure water used for the preparation of solutions was 59.7 mN/m. Equilibrium was obtained after 150 minutes, as shown in Figure 2.

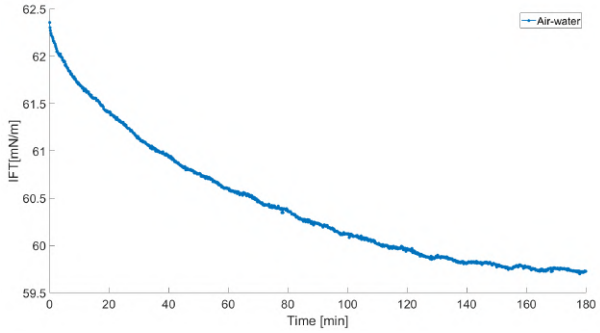

Figure 2. Air-water interfacial tension

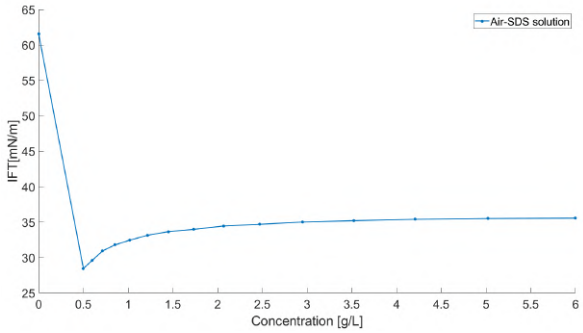

Figure 3. Air-SDS interfacial tension

Many factors influence the value of CMC, including temperature, pH, and the presence of organic modifiers. Taking the surface tension of SDS solutions as a function of concentration, the behavior expected was a sharp break at the CMC value, the surface tension decreases with increasing concentration until CMC is reached, after that becomes constant.

The measured equilibrium surface tension as a function of the surfactant concentration is presented in Figure 3. The interfacial tension value stabilizes at 34.4 mN/m. The surface tension drops dramatically as concentration rises until reaching a concentration close to 0,5g/L, at which point it begins to rise, resulting in a visible minimum in the surface tension curve.

This minimum in the surface tension value was also reported in other studies as El-Hefian and Yahaya (2011) and Miles and Shedlovsky (1944), and is explained by the presence of impurities that absorb at the air-liquid interface and have a surface activity greater than the surfactant itself. The impurities might be dodecyl alcohol or inorganic salts as SDS is not 100% pure.

2.1 Microfluidic micromodel

The flow through reservoir formation cannot be easily visualized. In order to visualize and study pore scale phenomena, transparent microfluidic devices representing a porous medium can be used.

Fluids like crude oil, surfactant and polymer solutions, and gases like air, carbon dioxide and nitrogen are introduced into these transparent micromodels using specific pumps. The resulting flow patterns and behaviors inside these devices are studied and analyzed.

The fluid injection experiments were performed on a microfluidic model porous medium, made with borosilicate glass and produced by Micronit (Figure 4). The micromodel is water-wet and has a porous matrix 20 mm long by 10 mm wide and 20μm etching-depth. Prior to the porous matrix, inlet and outlet channels act as flow distribution fractures that are 500 μm wide. The pore volume is 2.3 μL and matrix porosity is 57%. The permeability of the model, according to the supplier, is 2.5D.

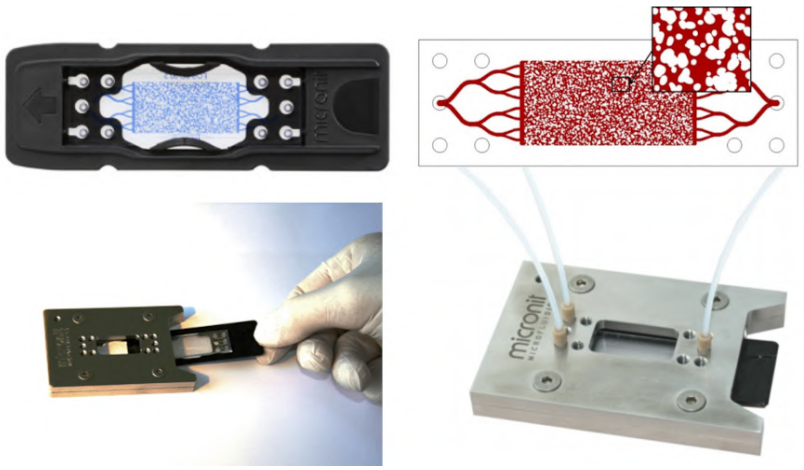

Figure 4. Micronit microfluidic device

The device was designed by randomly placing rock shape structures to resemble as much as possible the actual shape that is obtained by cutting a rock and scanning it. Throats and channels appear between the rock structures as a result of this random design. This approach of random placement provides no information about throat size distribution.

2.2 Experimental Setup

Since oil is absent in this study, it is a two-phase flow, with a gas phase and an aqueous phase, with or without surfactant. The fluid injection system (Figure 5) consisted of a syringe pump (Harvard Apparatus) used for injecting both phases. Fluid injection was performed using gas-tight glass syringes (Hamilton), the termination in Teflon with Luer-Lock coupling provides an easy connection with the 1/32" internal diameter tubing. A three-way valve was used to connect the pressure transducer.

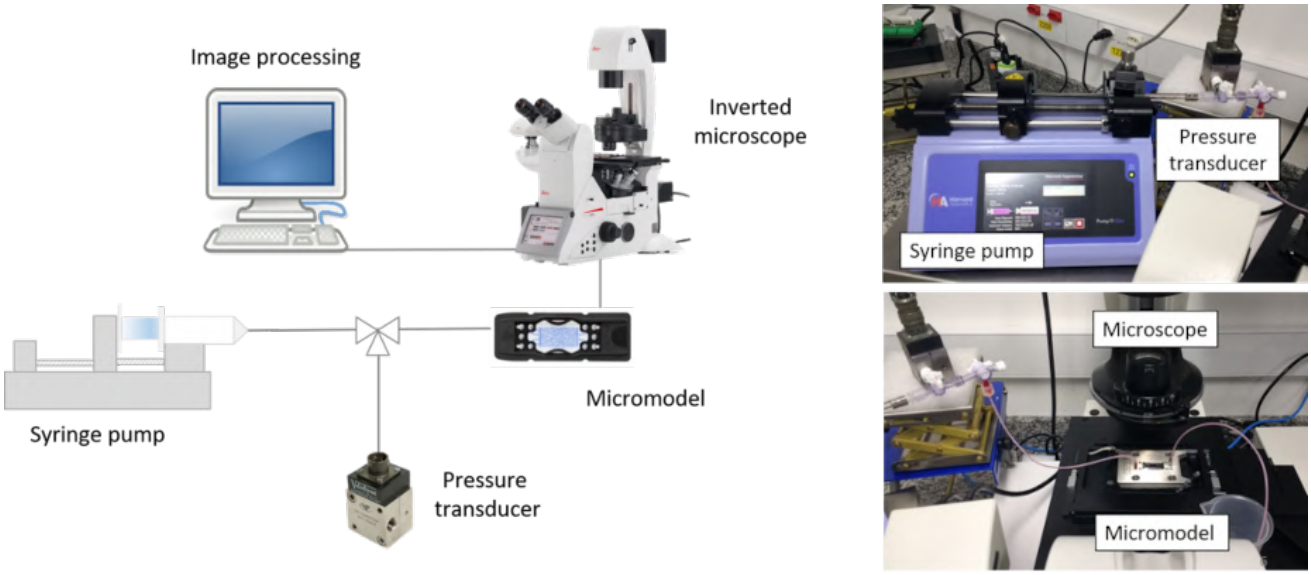

Figure 5. Experimental setup

The differential pressure was acquired using a DP15TL pressure transducer produced by Validyne Engineering placed between the syringe pump and the microfluidic device. The outlet was open to atmosphere and inlet pressure was measured during the test. In the plots the pressure will be shown as a normalized value defined as:

$$\bar{P}(t) = \frac{P(t) - P_{in}}{P_{in}} \tag{1}$$

in which P_{in} is the pressure value when the gas enters the micromodel.

The microfluidic device was placed on the stage of an inverted microscope (Leica DMi8) for visualization. Leica MC170 HD camera was used to record the evolution of the phase distribution during the experiment

2.3 Experimental procedure

In the experiments, the porous medium micromodel was initially saturated with pure water or a surfactant solution (SDS), then, gas-phase injection continued until the pressure reaches a steady-state condition. Air was injected at a constant volumetric flow rate, equal to 1ml/h. Surfactant concentration varied from 0g/L to 15.5g/L, the maximum concentration is approximately 54mM, 33$\times$CMC.

During gas injection and liquid displacement, multiple liquid films were formed. The recorded images of the phase distribution were processed in order to determine the characteristics of the gas and liquid flow, to assess the evolution of foam texture, and measure the number of lamellae in the pore space.

2.4 Image acquisition and processing

The image processing tool used to process the image was Fiji (Fiji Is Just ImageJ) that has built-in plugins that facilitates scientific image analysis. It is an open source package for a wide range of applications. The images used in the analysis were taken from a specific area of the microdevice (yellow rectangle), as shown in the Figure 6, for different time steps during the foam formation experiment.

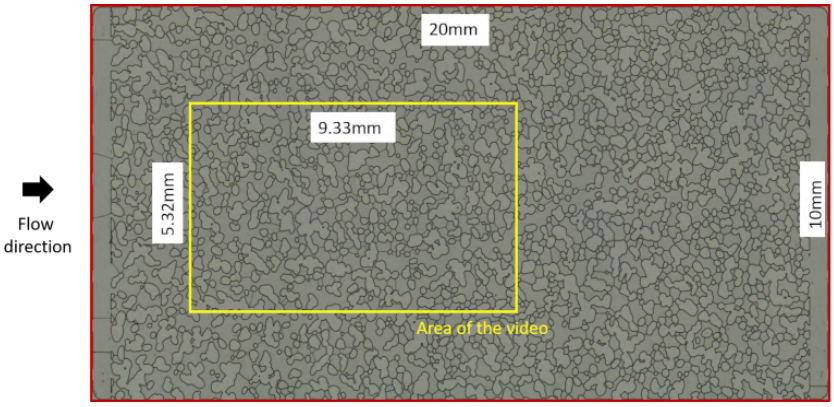

Figure 6. Area analyzed in the micromodel

The procedure used to determine the number of lamellae is discussed next. First, an image with the device completely saturated with air was used to define the configuration of the solid matrix and pore space (Figure 7).

During the surfactant solution displacement by gas injection, a frame obtained every 10 seconds of the video recorded was analyzed. Figure 8 presents an example of such image. The presence of liquid films defining multiple gas bubbles is clear.

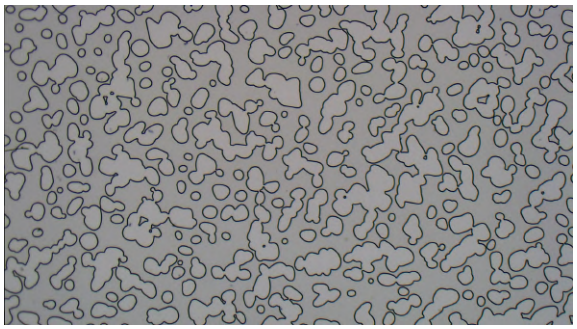

Figure 7. Device filled with air

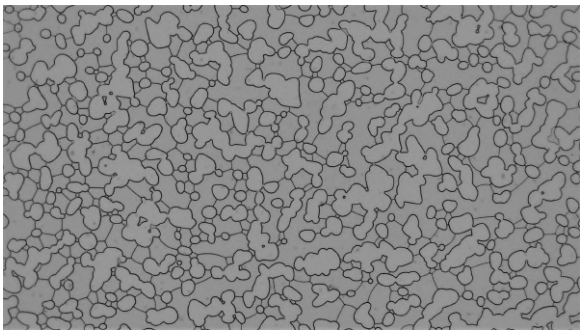

Figure 8. Device filled with liquid films (lamellae)

A plugin called bUnwarpJ was used to align the images, which is crucial for image subtraction operations that were used. The algorithm performs a simultaneous deformation in two images to make one look as similar as possible to the other.

A binarization procedure was performed using different automatic thresholds for both images. Examples are shown in Figure 9. Due to the differences in illumination between one experiment and another, different thresholds were tested; Default, Huang and Triangle. The choice of the best threshold for each test was made by comparing the number of lamellae obtained with the software with manual counting for all tests at different times. Spurious particles were also removed.

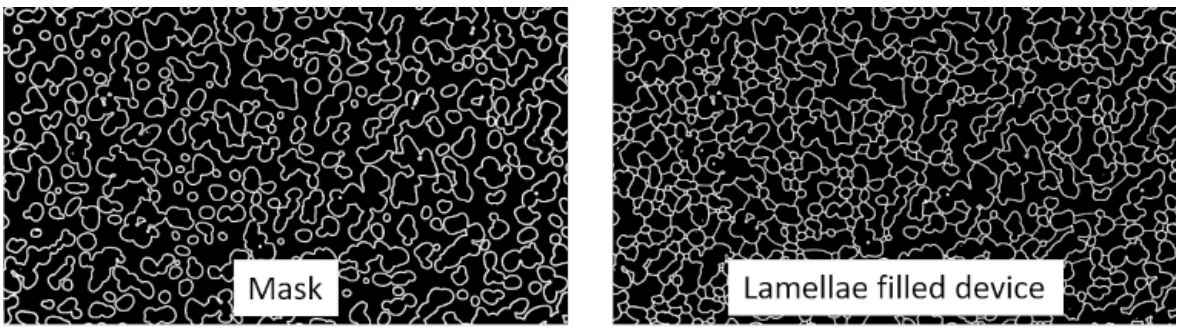

Figure 9. Binary images

A logical operation was performed between the binary, aligned images to remove the solid matrix and isolate the lamellae structures. Figure 10(A) shows an example of the result of such operations. Following step is called Skeletonize, in which pixels were repeatably removed from the edges of objects until they are reduced to single-pixel-wide shapes. In the skeletonized images, the nodes defined as the junction of two or more lamellae are identified and removed. Nodes are

marked by red circles in Figure 10(B).

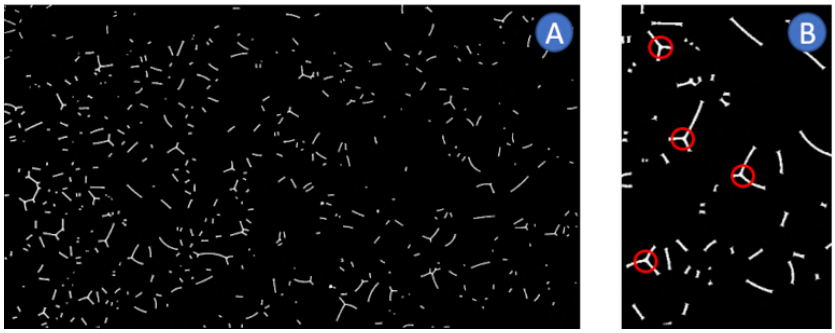

Figure 10. A)Lamellae identified by subtraction B)Nodes

The number of objects (lamellae) is then quantified for each frame and it is possible to build a graph with the evolution of the number of lamellae present in the observed area throughout the experiment. Figure 11 shows an example of an image with the counted lamellae, marked in red, over an image of the porous medium.

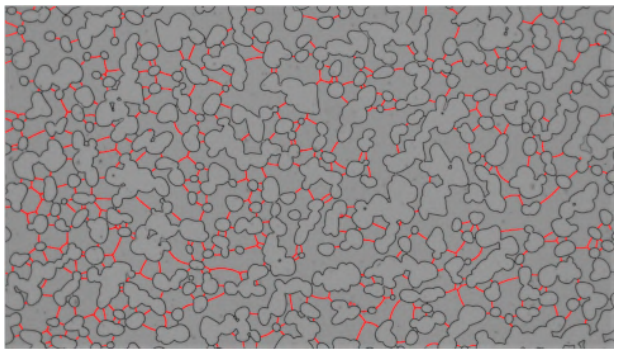

Figure 11. Lamellae marked in red

3. RESULTS AND DISCUSSION

The idea of the drainage experiments is to analyze the effect of surfactant concentration on foam formation.

3.1 Gas displacing pure water

As a base case, the first experiment consisted of pure water displacement by gas injection. The phase distribution after steady state is shown in Figure 12. Because of the very high viscosity ratio between the phases, the injected gas forms a preferential path that percolates the porous medium. The evolution of the inlet pressure is presented in Figure 13. The inlet pressure rises in the initial stages of the displacement process to overcome the capillary pressure and then falls as the lower viscosity phase (gas) displaces the higher viscosity phase (water). The inlet pressure reaches steady state after approximately 20 min (145 pore volumes).

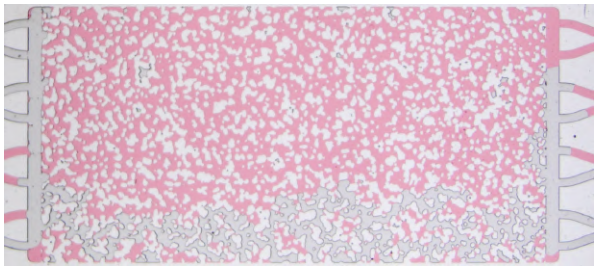

Figure 12. Saturation profile after gas injection - no surfactant added

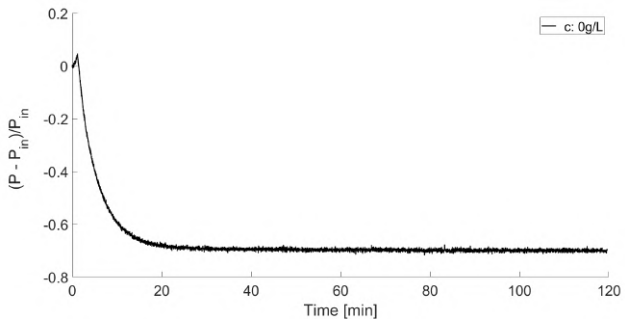

Figure 13. Normalized pressure behavior during gas injection - no surfactant added

Because of the relative high surface tension, foam is not formed in this experiment.

3.2 Gas displacing surfactant solution

Adding surfactant to the water completely changes the gas distribution inside the porous medium. At a concentration of c = 0.235g/L, below the CMC, a few liquid films are generated mostly by *leave-behind* mechanism. This mechanism creates lamellae parallel to the flow direction that provide little resistance to gas flow. This mechanism creates lamellae that are parallel to the flow direction, providing little resistance to gas flow.

The phase distribution at steady state is shown in Figure 14. The water saturation is much lower than in the pure water experiment. The mobility reduction of the gas phase led to flow diverging. Two main gas preferential paths can be observed in the figure.

The evolution of the inlet pressure is presented in Figure 15. As a basis of comparison, the inlet pressure for the pure water experiment is also shown. The pressure evolution in the initial stages of the process is the same. However, the inlet pressure stabilizes at a value higher than that observed in the pure water experiment. The higher value can be associated with the added resistance of the gas flow associated with the lamellae that were formed.

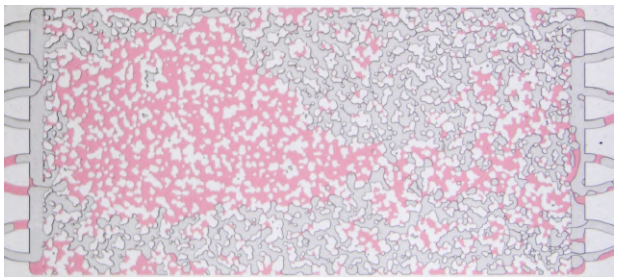

Figure 14. Saturation profile after gas injection (c = 0.235g/L)

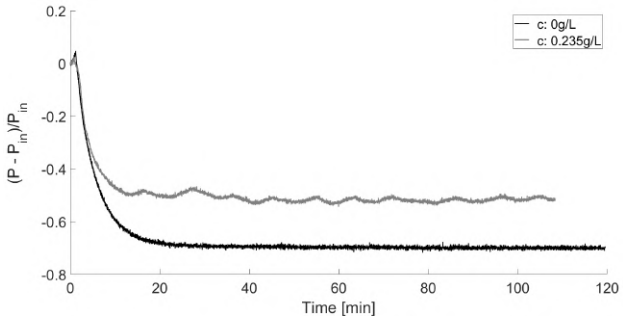

Figure 15. Normalized pressure behavior during gas injection

At the CMC, c = 0.47g/L, and above, the minimum pressure gradient to form strong foam is achieved. Gas flows discontinuously and the flow resistance of the liquid films formed contributes to an increase in the inlet pressure. At this condition, foam is formed not only by the *leave-behind* mechanism, but also by *snap-off*, *lamellae division* and *pinch-off*, as shown before.

Figure 16 presents the time evolution of the inlet pressure for different values of the surfactant concentration, up to approximately 3×CMC. The change in behavior is clear. For pure water and surfactant concentration close to 0.5×CMC (c = 0.235g/L), which was presented in Figure 15 and repeated in the plot as reference, the inlet pressure rises for a very short time and then falls quickly, until stabilizing at a value lower than the inlet pressure at the moment gas enters the porous medium.

The displacement of a surfactant solution with concentration equal to the CMC and above, the inlet pressure increase for a long time, reaches a maximum value and falls before reaching a steady-state plateau. The time and value of the maximum pressure rises with the surfactant concentration. At c = 0.47g/L (≈ CMC), the maximum pressure occurs at t≈20min (145 pore volumes); at c = 1.55g/L (≈ 3×CMC), the maximum pressure occurs at t≈40min (290 pore volumes).

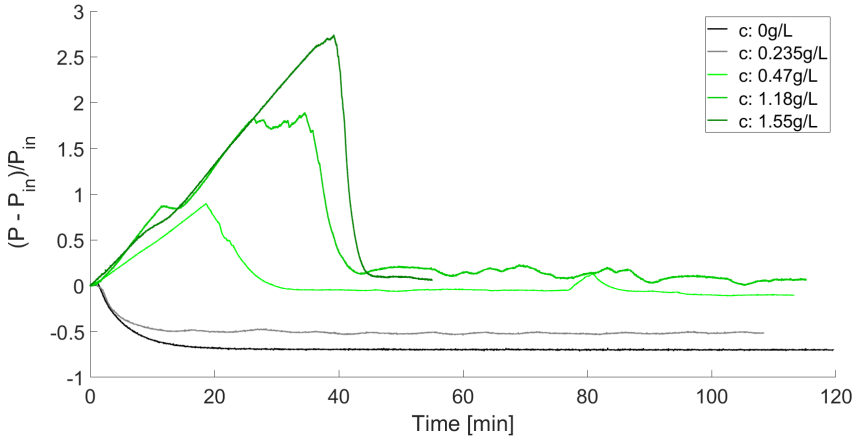

Figure 16. Normalized pressure behavior during gas injection - surfactant concentrations slightly above the CMC

The trend continues as the surfactant concentration increases even further. Figure 17 presents the inlet pressure evolution up to c = 15.5g/L (≈ 30×CMC). The value of the maximum pressure and the time it occurs still rises with surfactant

concentration. At c = 15.5g/L (≈ 30×CMC), the maximum pressure occurs at t≈10min (73 pore volumes).

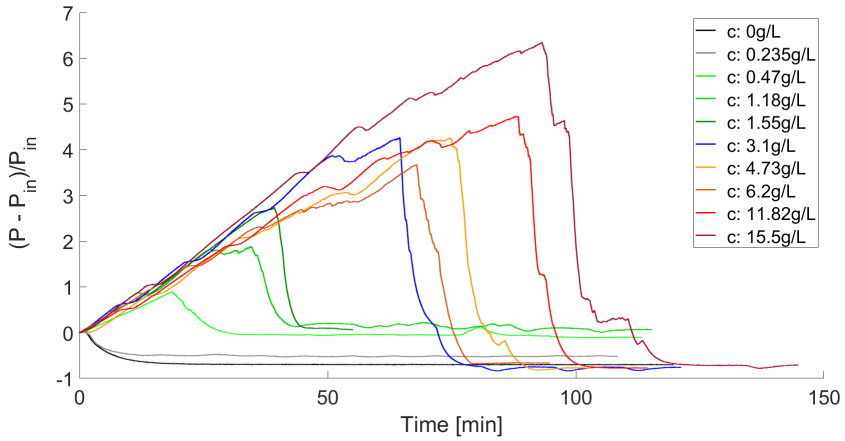

Figure 17. Normalized pressure behavior during gas injection

Foam strength can be determined by the inlet pressure measurements. Stronger foam, has a higher flow resistance that leads to higher inlet pressure.

Increasing the surfactant concentration to well above the CMC dramatically increases the pressure drop. Generating a more effective foam from a continuous gas foam requires mobilizing these lamellae so that they can multiply by lamella division and by repeated snap-off at the unoccupied pore throats. According to Aronson *et al.* (1994), strong foam in porous media with large flow resistance is produced by surfactant solutions with high repulsive disjoining pressures (higher surfactant concentration).

Rossen *et al.* (2017) studied the ability of foam to reduce gas mobility after a long period of gas injection. In a field test, one slug of surfactant solution was injected followed by months of gas injecting, they concluded that foam continued to reduce mobility by a modest amount even after long injection of gas. However, foam did weaken progressively as it dried out. They also commented that foam models assuming that foam remains strong at irreducible water saturation significantly overestimates foam effectiveness over extended periods of time. The reported behavior was also observed in the experiments presented here. At higher concentrations (well above the CMC) and high disjoining pressures, more lamellae can be created and a higher resistance is imposed to the gas flow represented by the increase in the pressure gradient.

It is important to note that the steady-state inlet pressure at the end of gas injection varies with the surfactant solution concentration. The results are summarized in Figure 18. For pure water and surfactant solution with concentration below the CMC, the dimensionless final inlet pressure is approximately $\bar{P}(t) = (P(t) - P_{in})/P_{in} \approx -0.8$. For surfactant concentration ∼1×CMC<c<∼3×CMC, the steady-state inlet pressure is higher, close to $\bar{P} \approx 0$. At higher surfactant concentration, the final dimensionless pressure is lower, close to $\bar{P} \approx -0.8$. At very high surfactant concentration, the formed lamellae are thinner and easier to be displaced, leading to a smaller final inlet pressure.

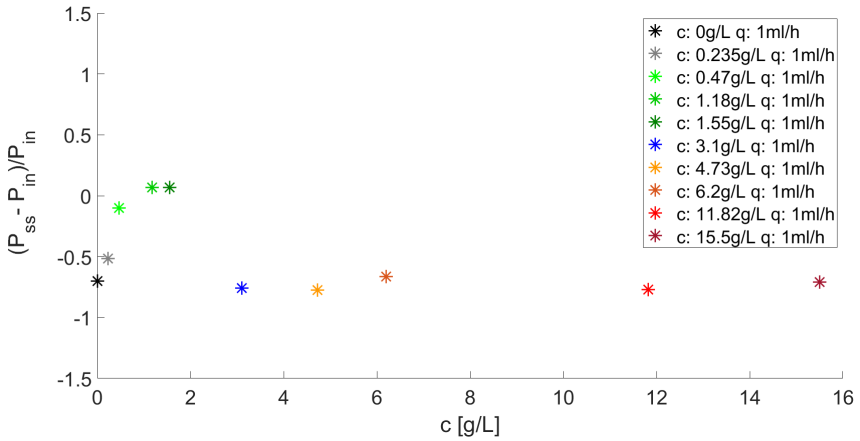

Figure 18. Pressure at steady state condition for different concentrations

Because of the lower mobility of the gas phase as foam is formed, the remaining water phase saturation at the end of the process falls as the surfactant concentration increases. The phase distribution at steady state for a surfactant concentration

of c = 0.47g/L is presented in Figure 19. The remaining water saturation (red phase) is much lower than that observed with pure water (Figure 12) and c = 0.235g/L (Figure 14).

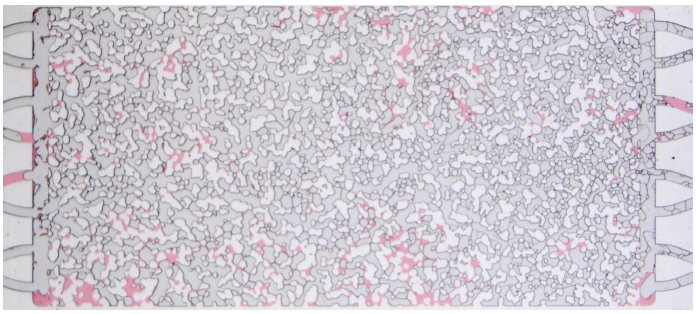

Figure 19. Saturation profile after gas injection - surfactant concentration at the CMC (c = 0.47g/L)

A large number of lamellae can be observed in the gas occupied pores. With a concentration even higher, water is present in the porous space only as thin films, forming the lamellae of the generated foam; as it is clear in Figure 20 (c = 1.18g/L).

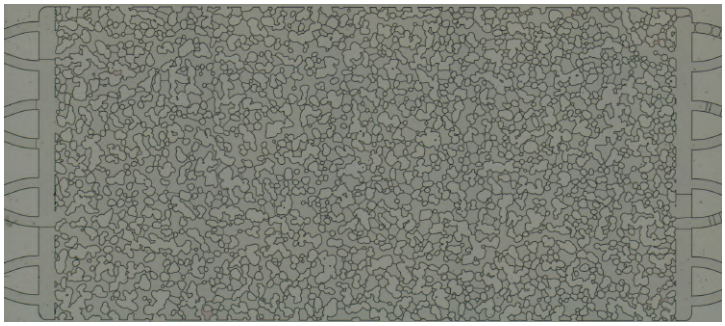

Figure 20. Saturation profile after gas injection - surfactant concentration slightly above the CMC (c = 1.18g/L)

The evolution of the lamella density as a function of time for different surfactant concentrations is shown in Figure 21. At steady state, the density was between 10 and $12/mm^2$ for all experiments, despite the different final inlet pressure.

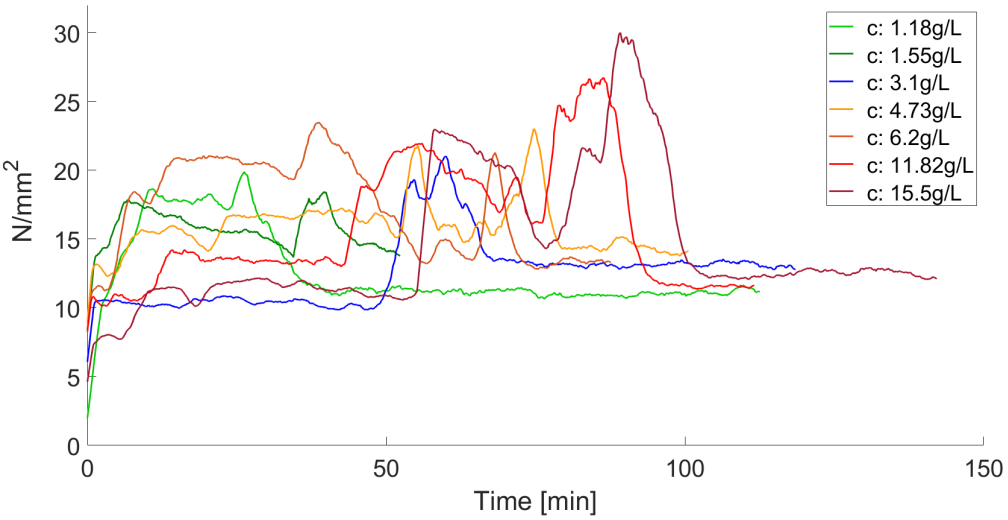

Figure 21. Lamellae number per millimeter square vs time

4. CONCLUSIONS

An investigation of foam formation in porous media using an anionic surfactant was described in this publication. Drainage tests were carried out and the conclusions are:

- The formation of gas foam films (lamellae) creates resistance to gas flow, increasing the magnitude of viscous forces against capillary forces.

- A minimum gradient pressure is required for strong foam formation.
- The pressure behavior do not depend only on the surface tension.
- The surfactant concentration alters lamellae population that compose foam, limiting the free motion of gas through the porous media.

5. ACKNOWLEDGEMENTS

The authors would like to acknowledge the funding agencies that contributed to this work: Capes (Coordenação de Aperfeiçoamento de Pessoal de Nível Superior), CNPq (Conselho Nacional de Desenvolvimento Científico e Tecnológico), Fulbright Doctoral Dissertation Research Abroad Award, ANP (Agência Nacional do Petróleo, Gás Natural e Biocombustíveis), Harvard University and Pontifical Catholic University of Rio de Janeiro (PUC-Rio). This study was financed in part by the Coordenação de Aperfeiçoamento de Pessoal de Nível Superior - Brasil (CAPES) - Finance Code 001

6. REFERENCES

Aronson, A., Bergeron, V., Fagan, M.E. and Radke, C., 1994. "The influence of disjoining pressure on foam stability and flow in porous media". *Colloids and Surfaces A: Physicochemical and Engineering Aspects*, Vol. 83, No. 2, pp. 109–120.

Blaker, T., Aarra, M.G., Skauge, A., Rasmussen, L., Celius, H.K., Martinsen, H.A. and Vassenden, F., 2002. "Foam for gas mobility control in the snorre field: the fawag project". *SPE Reservoir Evaluation & Engineering*, Vol. 5, No. 04, pp. 317–323.

Boud, D.C. and Holbrook, O.C., 1958. "Gas drive oil recovery process". US Patent 2,866,507.

Conn, C.A., Ma, K., Hirasaki, G.J. and Biswal, S.L., 2014. "Visualizing oil displacement with foam in a microfluidic device with permeability contrast". *Lab on a Chip*, Vol. 14, No. 20, pp. 3968–3977.

El-Hefian, E.A. and Yahaya, A.H., 2011. "Investigation on some properties of sds solutions". *Aust. J. Basic Appl. Sci*, Vol. 5, pp. 1221–1227.

Gauglitz, P.A., Friedmann, F., Kam, S.I. and Rossen, W., 2002. "Foam generation in porous media". In *SPE/DOE Improved Oil Recovery Symposium*. OnePetro.

Hirasaki, G., Jackson, R., Jin, M., Lawson, J., Londergan, J., Meinardus, H., Miller, C., Pope, G., Szafranski, R., Tanzil, D. *et al.*, 2000. "Field demonstration of the surfactant/foam process for remediation of a heterogeneous aquifer contaminated with dnapl". *NAPL Removal: Surfactants, Foams, and Microemulsions*, pp. 3–163.

Kahrobaei, S. and Farajzadeh, R., 2019. "Insights into effects of surfactant concentration on foam behavior in porous media". In *IOR 2019–20th European Symposium on Improved Oil Recovery*. European Association of Geoscientists & Engineers, Vol. 2019, pp. 1–13.

Kovscek, A.R. and Radke, C.J., 1993. "Fundamentals of foam transport in porous media".

Li, Q. and Prigiobbe, V., 2020. "Studying the generation of foam in the presence of nanoparticles using a microfluidic system". *Chemical Engineering Science*, Vol. 215, p. 115427.

Lin, S., 2008. *A computer simulation and molecular-thermodynamic framework to model the micellization of ionic branched surfactants in aqueous solution*. Ph.D. thesis, Massachusetts Institute of Technology.

Miles, G.D. and Shedlovsky, L., 1944. "Minima in surface tension–concentration curves of solutions of sodium alcohol sulfates." *The journal of physical chemistry*, Vol. 48, No. 1, pp. 57–62.

Portois, C., Boeije, C.S., Bertin, H.J. and Atteia, O., 2018. "Foam for environmental remediation: generation and blocking effect". *Transport in Porous Media*, Vol. 124, No. 3, pp. 787–801.

Rossen, W.R., Ocampo, A., Restrepo, A., Cifuentes, H.D. and Marin, J., 2017. "Long-time diversion in surfactant-alternating-gas foam enhanced oil recovery from a field test". *SPE Reservoir Evaluation & Engineering*, Vol. 20, No. 01, pp. 001–007.

Rossen, W., 1996. "Theory, measurements, and applications. foams".

Tanzil, D., Hirasaki, G. and Miller, C., 2002. "Conditions for foam generation in homogeneous porous media. paper spe 75176 presented at the spe/doe improved oil recovery symposium, tulsa, oklahoma, 13-17 april 2002".

7. RESPONSIBILITY NOTICE

The authors are solely responsible for the printed material included in this paper.